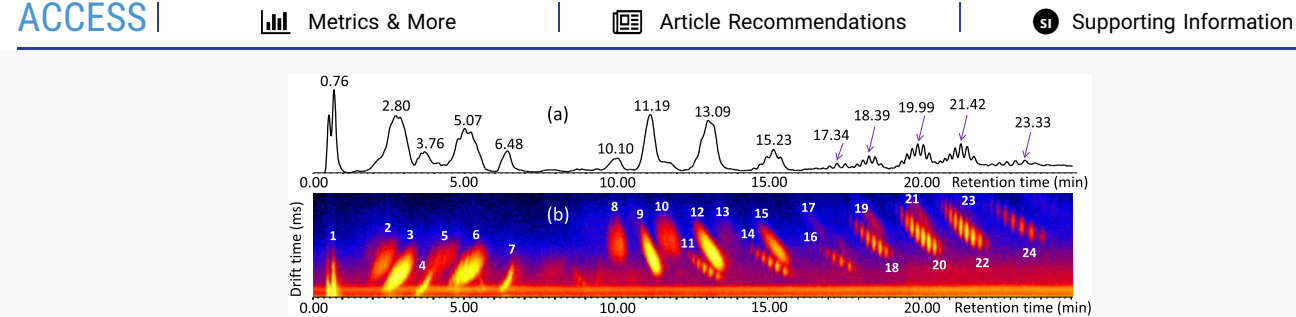


pubs.acs.org/ac Article

Multidimensional Mass Spectrometry of Multicomponent Nonionic Surfactant Blends

Jason M. O'Neill, Charles M. Johnson, and Chrys Wesdemiotis*





ABSTRACT: Ultraperformance liquid chromatography (UPLC) and ion mobility (IM) spectrometry were interfaced with mass spectrometry (MS) and tandem mass spectrometry (MS/MS) to characterize a complex nonionic surfactant mixture. The surfactant was composed of a glycerol core, functionalized with poly(ethylene oxide) units (PEO_n) that were partially esterified by caprylic and/or capric acid. Reversed-phase UPLC classified the blend based on polarity into four groups of eluates, corresponding to compounds with zero, one, two, or three fatty acid residues. Additional separation within each eluate group was achieved according to the length of the fatty acid chains. Coeluting molecules of similar polarity were dispersed in the gas phase by their collision cross section in the IM dimension. Performed in series, UPLC and IM allowed for the separation and detection of several isomeric and isobaric blend constituents, thereby enabling their isolation for conclusive MS/MS analysis to confirm or elucidate their primary structures and architectures (overall four-dimensional, 4D, characterization).

■ INTRODUCTION

Nonionic surfactants are amphiphilic compounds with high water solubility and low toxicity. They are commonly added to foods, cosmetics, pharmaceuticals, and other large-scale industrial mixtures as solubilizing agents, detergents, or emulsifiers.²⁻⁴ Basic nonionic surfactants are composed of aliphatic alcohols functionalized by a hydrophilic polymer, typically poly(ethylene oxide), PEO; widely used examples are fatty alcohol ethoxylates (FAEs) and alkylphenol ethoxylates (APEOs).⁵⁻⁷ More complex nonionic surfactants are composed of alcohol-containing cores like glycerol, sorbitan, or glucam;⁸⁻¹⁰ these cores are functionalized by a hydrophilic polymer (again, most commonly PEO) that is substituted (usually esterified) by a varying amount of fatty acids. This strategy creates a synthetic advantage by providing the ability to produce a diverse range of surfactant products from the same starting materials. Hydrophobicity is tuned using longer fatty acid chains, typically sourced from vegetable oil, whereas hydrophilicity is controlled by increasing the amount of PEO units (i.e., the degree of ethoxylation). You Understanding the composition of these complex mixtures is of paramount importance, as subtle variations in composition can cause significant changes in properties and performance.

Due to the compositional complexity of nonionic surfactant blends, their structural characterization requires analytical techniques that involve separation prior to detection. Since the surfactant constituents vary in polarity, they are ideally suited for fractionation by polarity-based techniques like gas chromatography (GC)^{12,13} and liquid chromatography (LC).14,15 Traditionally, these modes of separation have been paired with ultraviolet (UV), 16,17 refractive index (RI), 18 or evaporative light scattering (ELS) 19,20 detection. However, the latter methods lack selectivity and, hence, become inadequate with increasing mixture complexity. This issue is partly addressed by choosing mass spectrometry (MS) detection, which employs a molecule-specific property, viz., mass, for compound detection and identification. Indeed, GC-MS^{21,22} as well as LC-MS using high-performance liquid chromatography (HPLC), 8,23,24 ultraperformance liquid chromatography (UPLC), 10,25,26 or supercritical fluid chromatography (SFC)^{27,28} have all demonstrated success in characterizing these types of mixtures. Unfortunately, as mixture complexity continues to increase, so does the probability that multiple components have very similar polarities and, thus,

Received: June 17, 2021 Accepted: August 9, 2021



similar elution times. In these cases, ion mobility (IM) spectrometry offers an additional tool for orthogonal inline separation based on the charge and size/shape of the ionized LC eluates.²⁹ The IM dimension disperses by means other than polarity,^{30–32} which helps to resolve coeluting chromatography peaks. Such three-dimensional analysis has been performed on APEOs via SFC-IM-MS, resulting in increased resolution and peak identification.³³

In the present study, UPLC, IM separation, high-resolution MS detection, and subsequent tandem mass spectrometry (MS/MS) analysis via collisionally activated dissociation (CAD) are interfaced to carry out the first four-dimensional UPLC-IM-MS/MS characterization of a complex polymeric nonionic surfactant mixture. The product investigated is Chemonic CCG-6. The corresponding safety data sheet (SDS) reveals that this chemical contains a glycerol core, conjugated with an average of six ethylene oxide (EO) units (6 ethoxylations) and chain-end derivatized by a mixture of caprylic and capric fatty acid esters (cf. Figure 1).

$$R = \begin{cases} -C(=O)(CH_2)_6CH_3 & Caprylic (C_8) \\ -C(=O)(CH_2)_8CH_3 & Capric (C_{10}) \\ -H & O + CH_2CH_2O + R \\ R + OCH_2CH_2 + O + O + CH_2CH_2O + R \\ -OCH_2CH_2O + O + CH_2CH_2O + O + CH_2CH$$

Figure 1. Chemical structure of the nonionic surfactant Chemonic CCG-6. The glycerol core is functionalized by n ethoxylations (average n = 6), and the chain ends are derivatized by a varying number of caprylic and capric fatty acid ester groups.

EXPERIMENTAL SECTION

Materials. LC-MS-grade water, acetonitrile, formic acid, and ammonium acetate were obtained from Sigma-Aldrich (St. Louis, MO). Chemonic CCG-6, sold as "capric/caprylic glycerides," was obtained from The Lubrizol Corporation (Brecksville, OH). All materials were used as received.

Sample Preparation. For ESI-MS, 1.0 mg of CCG-6 was dissolved in 1 mL of MeOH. This solution was diluted with MeOH to a concentration of 1 ppb (μ g/kg) before injection into the ion source. For UPLC-IM-MS (MS/MS), 20 mg of analyte was dissolved in 1 mL of 50:50 H₂O/MeOH, and the resulting solution was diluted to 200 ppm (mg/kg) in 70:30 H₂O/MeOH and vortexed. The sample was filtered using an Acrodisc poly(vinylidene fluoride) (PVDF) syringe filter (13 mm, 0.2 μ m; Pall Corp, Port Washington, NY) into an LC–MS vial.

Liquid Chromatography. Reversed-phase LC separation was performed on a Waters Acquity UPLC system (Waters Corporation, Milford, MA) using a Phenomenex Luna Omega C_{18} 100 Å column ($100 \times 2.1 \text{ mm}^2$, $1.6 \mu \text{m}$ particle size) held at 50 °C. The run time was 30 min with a flow rate of 200 $\mu \text{L/min}$. Two mobile phases were employed (A and B); A consisted of $H_2\text{O}$ plus 0.1% (v/v) formic acid and B consisted of ACN plus 0.1% (v/v) formic acid. Separation was achieved by gradient and isocratic elution as follows: the initial mobile phase concentration of 40% B was gradually increased to 60% B over 8 min, then increased from 60% B to 70% B in 1 min, then increased to 95% in 11 min, where it was then held at 95% B for another 10 min. The volume of the sample injection

was 10 μ L. Post-column addition of 2.5 mM ammonium acetate in 50:50 ACN/H₂O at 100 μ L/min was utilized (adding this salt to the eluent would affect the eluent pH and peak resolution).

lon Mobility Mass Spectrometry. IM separation was achieved using traveling wave IM-MS^{10,31,32} and the following parameters: IM gas flow, 14.0 mL/min (N₂); traveling wave velocity, 500 m/s; and traveling wave height, 10 V.

Mass Spectrometry. The Acquity UPLC system was coupled to a Synapt G1 HDMS quadrupole/time-of-flight (Q/ToF) mass spectrometer (Waters Corporation, Milford, MA). The Q/ToF was operated in positive mode under the following optimized conditions: ESI capillary voltage, 3.0 kV; sample cone voltage, 30 V; extraction cone voltage, 3.0 V; source temperature, 120 °C; desolvation temperature, 250 °C; desolvation gas (N₂) flow, 500 L/h. MS spectra were acquired using ToF detection and Q in rf-only mode. MS/MS spectra were also acquired using ToF detection, however, with Q set in ion-selective mode to isolate the m/z of interest. During the MS/MS experiments, the collision voltage of the transfer cell was adjusted between 20 and 35 V, depending on the compound.

■ RESULTS AND DISCUSSION

ESI-MS Analysis. For initial screening, Chemonic CCG-6 was analyzed by single-stage ESI-MS (cf. Figure 2). Several

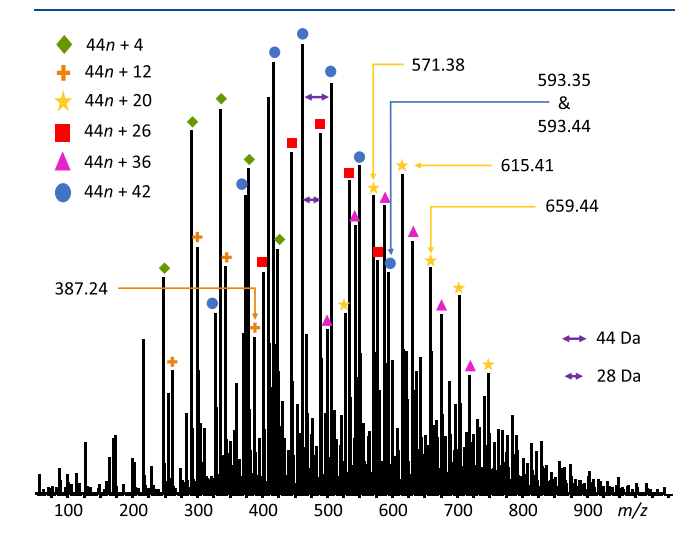


Figure 2. ESI-MS spectrum of CCG-6. All peaks represent sodiated ions

distributions are visible, attesting high complexity. Most intense peaks are separated by 44 or 28 Da, corresponding to the mass of the PEO repeat unit and the mass difference between caprylic and capric fatty acids, respectively. The CCG-6 name infers that the primary component of this blend contains a glycerol core, six EO units, and terminal caprylic and capric acid moieties. For brevity, this composition will be abbreviated as G-PEO₆-C₈C₁₀. When sodiated, [G-PEO₆-C₈C₁₀ + Na]⁺ has an m/z value of 659.44. While this peak is observed in the ESI-MS spectrum, it is neither the most intense nor the sole member within the G-PEO_n-C₈C₁₀ distribution (yellow stars), as G-PEO₅-C₈C₁₀ (m/z 615.41) and G-PEO₄-C₈C₁₀ (m/z 571.38) are also observed and in higher relative intensities. Another distribution, shifted 28 Da lower, arises from the replacement of a C₁₀ with a C₈ fatty acid,

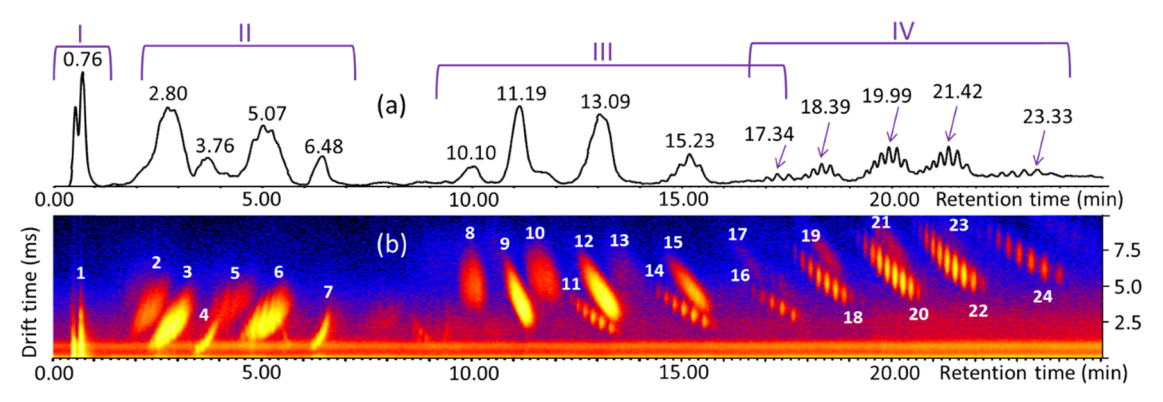


Figure 3. (a) UPLC-MS total ion chromatogram (TIC) and (b) LC-IM-MS total ion mobilogram of CCG-6. The retention times marked in the TIC correspond to the peak maxima. The compositions of distributions 1–24 are provided in Table S2 (see text for detailed identification).

which gives rise to the blend component G-PEO_n-C₈C₈ (pink triangles). These and all other ion distributions discerned in Figure 2 have been labeled by differently colored signs according to their nominal end group masses (E), which are derived from the measured m/z values via the equation m/z = $44n + E + Na^{+}$ (23 Da). Table S1 summarizes the elemental compositions of these and all other distributions detected in the CCG-6 sample. It is evident from this table that overlapping isomeric and isobaric blend components coexist, which further complicates the mass spectrum; for example, PEO₅-C₈ and G₂-PEO₁-C₁₀ are isomers with identical m/zratios for their Na⁺ adducts (387.24); whereas G-PEO₈-C₈ and G-PEO₁-C₈C₁₀C₁₀ are isobars with very similar m/z ratios for their sodiated forms (593.35 and 593.44, respectively). While single-stage ESI-MS analysis can give a general idea of the sample, it is clear that additional techniques are required for a more comprehensive characterization of the surfactant's composition. Such compounds can differ in four structural features: glycerol content, degree of ethoxylation, number of fatty acids, and identity of fatty acids. For complete assessment of all of these parameters, multidimensional (i.e., hyphenated) approaches are needed, as discussed in the following sections.

UPLC-IM-MS Three-Dimensional (3D) Characterization. The components of the CCG-6 surfactant blend differ in the proportion of their hydrophilic (glycerol and PEO) vs hydrophobic (fatty acid esters) segments, making reversedphase UPLC-MS ideally suitable for their chromatographic fractionation and identification. In reversed-phase UPLC, the stationary phase is nonpolar (C_{18} resin), while the mobile phase is polar. Under these conditions, a high glycerol content and/or degree of ethoxylation should decrease the retention time. Conversely, a larger number or length of fatty acid substituents should result in longer retention times. This trend is caused by favorable hydrophobic interactions between the fatty acid chains of the surfactant molecules and the structurally similar long alkyl chain functionality of the stationary phase on the column (C_{18}) . Using a combination of isocratic and gradient elution conditions, UPLC effectively separates the sample into 14 unique fractions (cf. Figure 3a). Unfortunately, coeluting distributions are apparent, as is evident from the large shoulders on the peaks eluting at 2.80 and 11.19 min, proving that UPLC alone does not have the resolving power necessary for such a complex surfactant mixture. To improve separation, the IM dimension was turned on. The result is the mobilogram depicted in Figure 3b. The overlay of mobilogram and chromatogram underscores the advantage of orthogonal two-dimensional (2D) separation by UPLC-IM-MS: the 14 distributions observed by UPLC are further dispersed into 24 distributions after UPLC-IM separation.

LC-IM-MS and LC-IM-MS/MS spectra were acquired after post-column addition of ammonium acetate to promote the formation of $[M+NH_4]^+$ ions. MS/MS of such species leads to structurally diagnostic dioxolanylium fragment ions that help to identify the fatty acid residue(s) attached to the ethoxylated glycerol segment. Furthermore, the presence of $[M+NH_4]^+$, $[M+Na]^+$, and $[M+H]^+$ ions in the LC-IM-MS mass spectra under these conditions helps to confidently deduce elemental composition based on three molecular species for the same oligomer.

Two-dimensional UPLC-IM separation significantly simplifies the resulting mass spectra, as illustrated in Figure 4 by

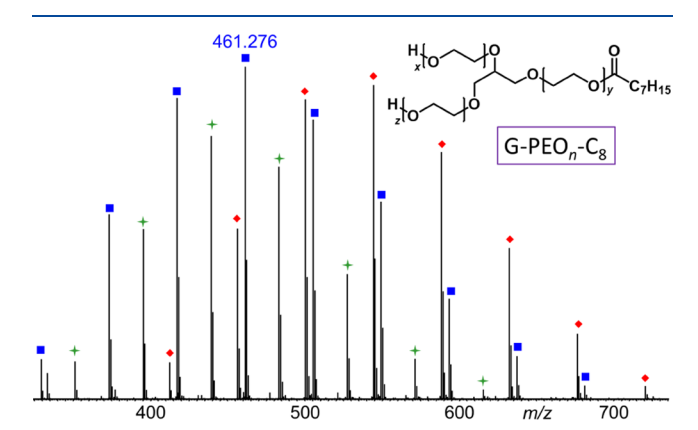


Figure 4. LC-IM-MS spectrum of distribution 3 in Figure 3b, displaying $G\text{-PEO}_n\text{-}C_8$ oligomers (44n + 42 Da), observed as [M + H]⁺ (green color star solid), [M + Na]⁺ (blue color box solid), and [M + NH₄]⁺ (red color tilted square solid) ions.

the LC-IM-MS spectrum of distribution 3. Exact mass measurement of the ions observed in this spectrum identifies distribution 3 as $G\text{-PEO}_n\text{-}C_8$ oligomers. The LC-IM-MS spectra of all distributions in Figure 3b are depicted in Figures S1–S24 and lead to the compositions summarized in Tables 1 and S2.

The LC-MS peaks (Figure 3a) can be divided into four distinct regions corresponding to the number of fatty acid moieties present. Region I (0–1 min) contains species with no fatty acid chains and thus minimal affinity for the column, which elute almost instantly (distribution 1 in the LC-IM-MS mobilogram). Region II contains six distinct distributions (2–

Table 1. Surfactant Constituents Identified by 3D LC-IM-MS Analysis

, , ,		
LC region	LC-IM distribution	composition ^a
I	1	$G\text{-PEO}_n$
II	2	G_2 -PEO _n - C_8
	3	G -PEO $_n$ -C $_8$
	4	PEO_n - C_8
	5	G_2 -PEO _n - C_{10}
	6	$G\text{-PEO}_n\text{-}C_{10}$
	7	PEO_n - C_{10}
III	8	G_2 -PEO _n - C_8C_8
	9	G -PEO $_n$ -C $_8$ C $_8$
	10	G_2 -PEO _n - C_8C_{10}
	11	PEO_n - C_8C_8
	12	$G-PEO_n-C_8C_{10}$
	13	G_2 -PEO _n - $C_{10}C_{10}$
	14	PEO_n - C_8C_{10}
	15	G -PEO $_n$ -C $_{10}$ C $_{10}$
	16	$PEO_n-C_{10}C_{10}$
IV	17	G_2 -PEO _n - $C_8C_8C_8$
	18	$G-PEO_n-C_8C_8C_8$
	19	G_2 -PEO _n - $C_8C_8C_{10}$
	20	G -PEO $_n$ -C $_8$ C $_8$ C $_{10}$
	21	G_2 -PEO _n - $C_8C_{10}C_{10}$
	22	$G\text{-PEO}_n\text{-}C_8C_{10}C_{10}$
	23	G_2 -PEO _n - $C_{10}C_{10}C_{10}$
	24	$G-PEO_n-C_{10}C_{10}C_{10}$

"See Table S2 for LC retention time, IM drift time, and m/z data. See Figures 4 and S1–S24 for the complete LC-IM-MS spectra.

7) eluting between 2 and 7 min, all containing one fatty acid chain. Region III, ranging from 9 to 18 min, includes nine distributions (8–16) of compounds with two fatty acid chains. Finally, eluting last in region IV are eight unique distributions (17–24) composed of compounds with three fatty acid chains.

Region I encompasses the oligomers labeled as distribution 1, which elute within 0.6–0.8 min. The LC-IM-MS spectrum identifies these species as ethoxylated glycerol, viz., G-PEO_n. Being highly polar and lacking any fatty acid substituent, these compounds interact minimally with the C₁₈ stationary phase and, thus, exit the column almost immediately with the void volume. The split nature of the LC peak (maxima at 0.64 and 0.76 min) is attributed to aggregation of the smaller oligomers via hydrogen bonding; such cluster formation reduces interactions with the hydrophobic stationary phase, resulting in quicker elution than the larger, nonaggregated chains. ¹⁰

The next eluates belong to region II, and all contain one fatty acid chain. Despite this common feature, further separation is achieved by LC-IM, revealing six distinct distributions in this region. Comparison of the TIC and mobilogram (Figure 3a,3b, respectively) highlights the utility of orthogonal separation by ion mobility. For example, a "single" peak is observed in the TIC at 2.80 min, but the mobilogram shows two unique distributions under this peak, 2 and 3. The elution time and drift time trends of the latter distributions give relevant information about their structures: their elution times indicate that distribution 2 should be more polar than distribution 3, while their drift times point out that distribution 2 must have a larger collision cross section than 3.31,32 Based on accurate mass measurements (Table S2), distributions 2 and 3 are composed of G₂-PEO_n-C₈ and G- PEO_n - C_8 molecules, respectively. These structures agree well

with the predictions from LC and IM, as an additional glycerol unit should increase both polarity and collision cross section. Continuing this logic, distribution 4 must be less polar and smaller in collision cross section than 2 and 3, in full agreement with the structure PEO_n-C₈ revealed by accurate mass measurement (Table S2); this compound is a side product with no glycerol content. A closer look at the mobilogram shows that distributions 5, 6, and 7 appear strikingly similar to 2, 3, and 4, respectively, the only difference being their higher elution times. This increase is reconciled if distributions 5-7 are the C₁₀ fatty ester analogues of distributions 2-4. A C₁₀ chain interacts more favorably with the C₁₈ stationary phase, causing a later elution. This pattern is important to notice as it aids in the identification of later eluting species. Accordingly, the elution time, drift time, and accurate mass data of distributions 5, 6, and 7 corroborate the molecular structures G_2 -PEO_n- C_{10} , G-PEO_n- C_{10} , and PEO_n- C_{10} , respectively.

The next surfactant constituents to elute belong to region III; they contain two fatty acid tails, which increases the complexity of chromatographic separation. Compounds with one tail (region II) include either a C_8 or a C_{10} chain end; however, with two tails (region III), the potential chain-end combinations become C₈C₈, C₈C₁₀, and C₁₀C₁₀. According to reversed-phase LC theory, compounds with two C₈ tails should elute first. Hence, distribution 8 (first in region III) is assigned to G_2 -PEO_n- C_8C_8 . The corresponding C_8C_{10} and $C_{10}C_{10}$ diglycerol analogues are identified in successive eluates, as distributions 10 and 13, respectively. On the other hand, the monoglycerol congeners G-PEO_n-C₈C₈, G-PEO_n-C₈C₁₀, and G-PEO_n-C₁₀C₁₀ are detected in distributions 9, 12, and 15, respectively, each eluting after the diglyceride with the same ester combination due to the higher hydrophobicity of G vs G2 containing species (cf. Tables 1 and S2). Finally, distributions 11, 14, and 16 in region III correspond to PEO_n-C₈C₈, PEO_n- C_8C_{10} , and PEO_n- $C_{10}C_{10}$; the lack of a glycerol core in these products allows for additional interactions with the C₁₈ stationary phase, resulting in superior chromatographic separation between differently esterified PEO_n oligomers. Region III underlines the importance of the orthogonal IM separation. What appears to be 4 or 5 peaks in the LC chromatogram is clearly shown to contain 9 unique distributions with the assistance of the IM dimension.

Finally, eluting last in region IV are surfactant constituents with three fatty acid tails. The noticeable appearance of four broad LC peaks, all showing partially resolved oligomers, arises from the possible fatty acid tail combinations of C₈C₈C₈, $C_8C_8C_{10}$, $C_8C_{10}C_{10}$, and $C_{10}C_{10}C_{10}$. In accordance with the previous regions, the first distribution (17) to elute is the most polar diglycerol, in this case G₂-PEO_n-C₈C₈C₈. The more hydrophobic tri-esterified diglycerol analogues G2-PEOn- $C_8C_8C_{10}$, G_2 -PEO_n- $C_8C_{10}C_{10}$, and G_2 -PEO_n- $C_{10}C_{10}C_{10}$ are identified as distributions 19, 21, and 23 respectively. As expected, the more intense distributions in region IV, viz., 18, 20, 22, and 24, originate from the corresponding tri-esterified monoglycerol products G-PEO_n-C₈C₈C₈, G-PEO_n-C₈C₈C₁₀, $G-PEO_n-C_8C_{10}C_{10}$, and $G-PEO_n-C_{10}C_{10}C_{10}$, respectively. It is evident from the TIC and mobilogram in Figure 3 that the third fatty acid moiety increases retention on the stationary phase, resulting in chromatographic separation of individual PEO oligomers. Overall, 2D LC-IM dispersion separated several coeluting compounds (cf. Figure 3a vs b), including isomers (4 vs 5, 10 vs 11, and 13 vs 14), and isobars (for example, 2 vs 21 or 6 vs 24).

UPLC-IM-MS/MS Four-Dimensional (4D) Structure Verification. To confirm the proposed structures derived by UPLC-IM-MS, a specific oligomer from each LC-IM distribution was subjected to MS/MS analysis via collisionally activated dissociation (CAD) (cf. Figures 5 and S25–S47).

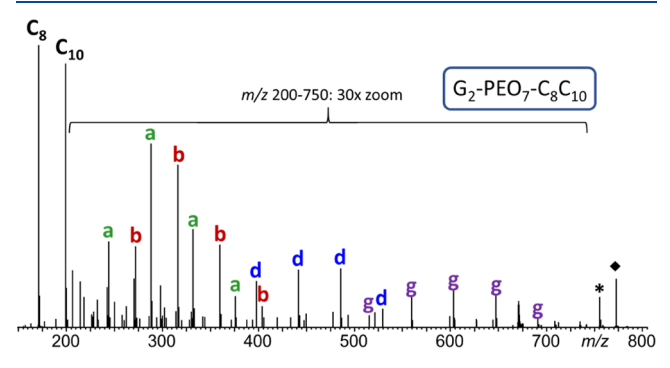


Figure 5. LC-IM-MS/MS spectrum of the $[M + NH_4]^+$ ion from G_2 - PEO_7 - C_8C_{10} (m/z 772.539; marked by \spadesuit). See Scheme S3 for a key to the fragment ion labels.

Ammoniated molecules were selected in these experiments, as they provided structurally diagnostic MS/MS spectra. A fragmentation observed consistently for all [M + NH₄]⁺ precursor ions is the cleavage of the fatty acid tail plus the adjoining ethylene oxide unit to form a dioxolanylium ion (cf. Scheme S1). 8,10,34 This process results in the observation of dioxolanylium ions characteristic for either caprylic acid (m/z)171.14) or capric acid (m/z 199.16); such fragments readily identify the fatty acid(s) present in the selected n-mer, as demonstrated in Figure 5 by the LC-IM-MS/MS spectrum of ammoniated G_2 -PEO₇- C_8C_{10} (m/z 772.54). In keeping with the composition of this molecule, both caprylic and capric dioxolanylium ions are observed (denoted by C₈ and C₁₀, respectively, in the spectrum). It is further noteworthy that the intensity ratio of the dioxolanylium peaks is similar to the ratio of the corresponding fatty acids in the selected n-mer. This observation is affirmed by the MS/MS spectra of G₂-PEO₇- $C_8C_8C_{10}$ (Figure S42) and G_2 -PEO₇- $C_8C_{10}C_{10}$ (Figure S44), where the intensity ratio of the C₈ and C₁₀ peaks is approximately 2:1 in the former, but approximately 1:2 in the latter spectrum, consistent with the caprylic/capric acid ratios in these tri-esterified species. Moreover, C₈ or C₁₀ peaks are insignificant if there is no C_8 or C_{10} substituent, respectively (cf. MS/MS spectra of PEO₅-C₈C₈, G-PEO₅-C₈C₁₀, and G₂-PEO₈-C₁₀C₁₀ in Figures S34-S36, respectively).

A second type of MS/MS fragments observed from all oligomers with glycerol core(s), albeit with much lower relative intensities, are reconciled by C–O bond dissociations in the PEO/glycerol chains, as rationalized in Schemes S2 and S3. It should be noted that these fragments appear as protonated ions, suggesting that their formation is accompanied by NH₃ loss (as shown in Schemes S2 and S3) or proceeding from the [M + H]⁺ ion created by initial loss of NH₃ (denoted with an asterisk in the spectra). Charge-induced ether bond scissions (Scheme S2) account for the formation of fragments with terminal vinyl or hydroxy groups. ³⁵ Conversely, charge-remote ester bond scissions, proceeding through 1,5-hydrogen rearrangement to the carbonyl group (Scheme S3), provide an alternative pathway to fragments with vinyl chain ends. ³⁵ Once formed, vinyl-terminated PEO chains may undergo

consecutive depolymerization under CAD conditions (cf. Scheme S4). These reactions can generate the fragment series \mathbf{a} — \mathbf{h} listed in Table S3; what products are actually observed is dictated by the structure of the selected molecule. For example, the G_2 -PEO $_7$ - C_8C_{10} oligomer depicted in Figure 5 gives rise to the four fragment series labeled \mathbf{a} , \mathbf{b} , \mathbf{d} , and \mathbf{g} (cf. Scheme S5). Series \mathbf{a} and \mathbf{b} correspond to fragments with the connectivity \mathbf{G} -PEO $_n$ - \mathbf{C}_8 and \mathbf{G} -PEO $_n$ - \mathbf{C}_{10} , further corroborating the presence of both caprylic and capric fatty acids within this n-mer. Fragment series \mathbf{d} corresponds to \mathbf{G} -PEO $_n$ - \mathbf{C}_8C_{10} , formed via the loss of a glycerol and its EO units; it verifies that unesterified PEO branches are present in the analyzed oligomer. Finally, the peaks denoted with \mathbf{g} have the composition \mathbf{G}_2 -PEO $_n$ - \mathbf{C}_8C_{10} , validating the inclusion of two glycerol units in this surfactant component.

CONCLUSIONS

Nonionic surfactant mixtures benefit from structural complexity, as a diverse range of hydrophilic and hydrophobic groups also endows a wide range of physical properties. Unfortunately, this complexity makes a full characterization difficult to accomplish. Our study demonstrated the analytical power of 4D UPLC-IM-MS/MS by successfully separating and identifying the components of the widely used nonionic surfactant Chemonic CCG-6. UPLC facilitated separation based on the type and amount of fatty acid esters in the sample, revealing 14 distributions. Combined with orthogonal IM dispersion, which facilitated separation based on glycerol content, a total of 24 unique distributions were conclusively identified by accurate measurement of >500 m/z values. The structures derived this way were further confirmed by the MS/MS analysis of individual oligomers within each of the 24 distributions. This combination of four techniques (UPLC, IM, MS, and MS/ MS), in 4D inline mode, was successfully applied for the first time to a surfactant blend. Future work will combine this methodology with the use of internal standards that cover the polarity range of nonionic surfactants to also allow for quantitative analysis of the mixture components, which are expected to vary widely in ionization efficiency.

ASSOCIATED CONTENT

Supporting Information

The Supporting Information is available free of charge at https://pubs.acs.org/doi/10.1021/acs.analchem.1c02551.

Observed polymeric distributions and their LC, IM, and m/z data; labels in MS/MS spectra; LC-IM-MS spectra of the 24 product distributions characterized; LC-IM-MS/MS spectra of specific oligomers from each of the product distributions; and fragmentation pathways observed in the MS/MS experiments (PDF)

AUTHOR INFORMATION

Corresponding Author

Chrys Wesdemiotis — Department of Chemistry, The University of Akron, Akron, Ohio 44325, United States; orcid.org/0000-0002-7916-4782; Email: wesdemiotis@uakron.edu

Authors

Jason M. O'Neill – Department of Chemistry, The University of Akron, Akron, Ohio 44325, United States

Charles M. Johnson – Department of Chemistry, The University of Akron, Akron, Ohio 44325, United States

Complete contact information is available at: https://pubs.acs.org/10.1021/acs.analchem.1c02551

Notes

The authors declare no competing financial interest.

ACKNOWLEDGMENTS

Support from the National Science Foundation (CHE-1808115) is gratefully acknowledged. The authors thank Lubrizol Corporation for providing a sample of CCG-6.

REFERENCES

- (1) Porter, M. R. *Handbook of Surfactants*, 2nd ed.; Blackie Academic & Professional: London, 1994.
- (2) Jiao, J. Adv. Drug Delivery Rev. 2008, 60, 1663-1673.
- (3) Tadros, T. F. An Introduction to Surfactants; De Gruyter: Berlin, Germany, 2014.
- (4) Cosmetic Science and Technology: Theoretical Principles and Applications, 1st ed.; Sakamoto, K.; Lochhead, R.; Maibach, H.; Yamashita, Y., Eds.; Elsevier: Amsterdam, 2017.
- (5) O'Lenick, A. J.; Parkinson, J. K. J. Am. Oil Chem. Soc. 1996, 73, 63–66.
- (6) Dunphy, J. C.; Pessler, D. G.; Morrall, S. W.; Evans, K. A.; Robaugh, D. A.; Fujimoto, G.; Negahban, A. *Environ. Sci. Technol.* **2001**, *35*, 1223–1230.
- (7) Luo, X.; Zhang, L.; Niu, Z.; Ye, X.; Tang, Z.; Xia, S. J. Chromatogr. A 2017, 1530, 80-89.
- (8) Solak Erdem, N.; Alawani, N.; Wesdemiotis, C. *Anal. Chim. Acta* **2014**, *808*, 83–93.
- (9) Santos, J.; Calero, N.; Muñoz, J. Chem. Eng. Res. Des. **2015**, 100, 261–267.
- (10) Katzenmeyer, B. C.; Hague, S. F.; Wesdemiotis, C. *Anal. Chem.* **2016**, *88*, 851–857.
- (11) Nonionic Surfactants: Organic Chemistry, Van Os, N. M., Ed.; Marcel Dekker, Inc.: New York, 1998.
- (12) Szymanowski, J. Crit. Rev. Anal. Chem. 1990, 21, 407-451.
- (13) Nace, V. M.; Knoell, J. C. J. Am. Oil Chem. Soc. 1995, 72, 89-95.
- (14) Escott, R. E. A.; Brinkworth, S. J.; Steedman, T. A. J. Chromatogr. A 1983, 282, 655–661.
- (15) Plaza, M.; Pons, R. Colloids Surf. A 1998, 137, 287-293.
- (16) Carrion, J. L.; Sagrado, S.; de la Guardia, M. Anal. Chim. Acta 1986, 185, 101–107.
- Hoffman, B. J.; Taylor, L. T.; Rumbelow, S.; Goff, L.; Pinkston,
 J. D. J. Chromatogr. A 2004, 1034, 207–212.
- (18) Trathnigg, B. J. Chromatogr. A 2001, 915, 155-166.
- (19) Martin, N. J. Liq. Chromatogr. 1995, 18, 1173-1194.
- (20) Park, H. S.; Ryu, H. R.; Rhee, C. K. Talanta 2006, 70, 481-484.
- (21) Cserháti, T.; Forgács, E. J. Chromatogr. A 1997, 774, 265-279.
- (22) Wulf, V.; Wienand, N.; Wirtz, M.; Kling, H. W.; Gäb, S.; Schmitz, O. J. J. Chromatogr. A 2010, 1217, 749-754.
- (23) Scullion, S. D.; Clench, M. R.; Cooke, M.; Ashcroft, A. E. J. Chromatogr. A **1996**, 733, 207–216.
- (24) Levine, L. H.; Garland, J. L.; Johnson, J. V. Anal. Chem. 2002, 74, 2064–2071.
- (25) Lara-Martín, P. A.; González-Mazo, E.; Brownawell, B. J. Anal. Bioanal. Chem. 2012, 402, 2359–2368.
- (26) Tush, D.; Loftin, K. A.; Meyer, M. T. J. Chromatogr. A 2013, 1319, 80–87.
- (27) Pinkston, J. D.; Marapane, S. B.; Jordan, G. T.; Clair, B. D. J. Am. Soc. Mass Spectrom. **2002**, 13, 1195–1208.
- (28) Pan, J.; Tang, Y.; Shen, Z.; Du, Z. J. Mass Spectrom. 2020, 55, No. e4499.

- (29) Cumeras, R.; Figueras, E.; Davis, C. E.; Baumbach, J. I.; Gràcia, I. *Analyst* **2015**, *140*, 1376–1390.
- (30) Snelling, J. R.; Scarff, C. A.; Scrivens, J. H. Anal. Chem. 2012, 84, 6521-6529.
- (31) Ion Mobility Spectrometry Mass Spectrometry: Theory and Applications, Wilkins, C. L.; Trimpin, S., Eds.; CRC Press: Boca Raton, FL, 2010.
- (32) Wesdemiotis, C. Angew. Chem., Int. Ed. 2017, 56, 1452-1464.
- (33) Ma, Q.; Zhang, Y.; Zhai, J.; Chen, X.; Du, Z.; Li, W.; Bai, H. Anal. Bioanal. Chem. **2019**, 411, 2759–2765.
- (34) Borisov, O. V.; Ji, J. A.; Wang, Y. J.; Vega, F.; Ling, V. T. Anal. Chem. **2011**, 83, 3934–3942.
- (35) Wesdemiotis, C.; Solak, N.; Polce, M. J.; Dabney, D. E.; Chaicharoen, K.; Katzenmeyer, B. C. *Mass Spectrom. Rev.* **2011**, *30*, 523–539.